Application of Wave Based Technique for a cavity considering forced excitation at boundaries and effects of absorption materials

A. Hepberger, F. Diwoky, K. Jalics, H.-H. Priebsch
ACC Acoustic Competence Center G.m.B.H.
Inffeldgasse 25, A-8010 Graz, Austria
email: **achim.hepberger@accgraz.com**

Abstract
The Wave Based Technique (WBT) is a novel prediction technique for steady-state acoustic analysis, which is based on the indirect Trefftz approach. Recently, a methodology has been developed, which allows to consider a 3-dimensional fluid domain with prescribed normal velocity and prescribed normal impedance boundary conditions. For this methodology, it is necessary that the acoustic problem domain is convex.
To extend the application field of the WBT methodology a new prescribed velocity boundary condition is introduced in order to consider the structural local distribution of vibration velocities at the boundaries. The velocity distributions can be derived from either measurement data or from results of structural FEM analyses. By using this new boundary condition the excitation of the fluid due to structural vibrations can be considered. For validation purposes, a car-like cavity (Sound Brick) was designed. Results of FEM calculations and measurements were compared to those of the WBT.

1 Introduction

A modern vehicle development process requires efficient and precise prediction techniques for the vehicle interior noise. Disadvantages and restrictions still exist for well introduced methods. On the one hand, the Finite Element Method (FEM) is a standard for vibro-acoustic simulations in the lower frequency range. But there are limitations in effort and precision at higher frequencies. Especially for passenger car cavities, the computation effort can be unacceptable above 300 Hz, due to the need of mesh refinement.
On the other hand, Statistical Energy Analysis (SEA) has been applied with success for car interior noise prediction at higher frequencies. Here, the limits exist due to reduced quality of the results at lower frequencies (below about 400 – 600 Hz) and due to reduced modal density of structures and acoustic domains. Furthermore, SEA has the general disadvantage, that no phase information is available, which usually is still important in the frequency range described.

In order to predict noise in structural and acoustic domains in a wider frequency range, the Wave Based prediction Technique (WBT) has been developed as an alternative to other methods [1]. The advantage of WBT is seen in covering the whole frequency range of automotive noise simulation applications in one and to close the above described prediction gap between FEM and SEA. Based on the theory and first principle applications [4], an efficient implementation has been developed for multi-domain 3D acoustic problems [2], [6] and simulation results have been validated with measurements under echoic conditions and considering absorbing materials positioned in a test cavity [5].

For practical applications, local velocity distributions as generated by vibrating boundaries of a cavity have to be considered. Consequently, this paper describes, how such prescribed boundary conditions can be handled for a local velocity field generated by FEM or measurement. Furthermore, verification

examples of simulation results are shown for a specifically developed test set-up and the efficiency of the WBT compared to FEM is discussed for test application including absorption effects.

2 Basic concepts of the Wave Based Technique

The WBT is a deterministic method and is based on the indirect Trefftz approach [3], in that the dynamic field variables in the problem domain are expressed in terms of wave functions, which are solutions the governing dynamic equations. These field variables of the wave function expansions satisfy the governing dynamic equations exactly. Only the boundary conditions are not a priori satisfied. By enforcing the solution expansions to satisfy the boundary conditions in an integral sense, a linear wave model is obtained. The contribution factors of the wave functions to the solutions form the degrees of freedom (DOF) of a wave model.

As shown in [1] the convexity of the problem domains is a sufficient condition for the proposed solution expansion to converge towards to the exact solution. For non-convex problem domains, domain decomposition into convex sub-domains is required. For more details about the theoretical background of the WBT concept and multi-domain acoustic problems, the reader is referred to [4], [5].

2.1 Problem definition

The 3D acoustic problem, as shown in Figure 1, is considered. Expect for the floor surface Ω_Z, at which a normal impedance boundary condition is applied and for the front surface Ω_{v1}, at which a normal velocity boundary condition is applied and excites the cavity, all the boundary surfaces Ω_{v0} of the acoustic cavity $V = \left(L_x, L_y, L_z\right) = \left(4.02, 1.4, 1.7\right) m$ are assumed to be perfectly rigid. Inside the cavity a fluid is characterized by a speed of sound ($c = 344.385 m/s$), an ambient density ($\rho = 1.1958 kg/m^3$) and an ambient temperature ($T = 21°C$).

The steady-state pressure response $p(\mathbf{r}) = (x, y, z)$ inside the cavity V governed by the homogenous Helmholtz equation

$$\left(\Delta + k^2\right) p(\mathbf{r}) = 0, \qquad \forall \mathbf{r} \in V \tag{1}$$

with the Laplace operator $\Delta = \frac{\partial^2}{\partial x^2} + \frac{\partial^2}{\partial y^2} + \frac{\partial^2}{\partial z^2} = \nabla^2$, the acoustic wave number $k = \omega / c$ and the circular frequency ω.

The boundary conditions are defined as follows:

$$\frac{j}{\rho\omega}\frac{\partial p(\mathbf{r})}{\partial n} = \frac{p(\mathbf{r})}{\overline{Z}_n}, \qquad \forall \mathbf{r} \in \Omega_Z \tag{2}$$

$$\frac{j}{\rho\omega}\frac{\partial p(\mathbf{r})}{\partial n} = \overline{v}_n, \qquad \forall \mathbf{r} \in \Omega_{v1} \tag{3}$$

$$\frac{j}{\rho\omega}\frac{\partial p(\mathbf{r})}{\partial n} = 0, \qquad \forall \mathbf{r} \in \Omega_{v0} \tag{4}$$

where $\overline{Z}_n$ represents the prescribed normal impedance, $\overline{v}_n$ the prescribed normal velocity, $j = \sqrt{-1}$ the unit imaginary number and $\partial / \partial n$ the derivative in the outward normal direction.

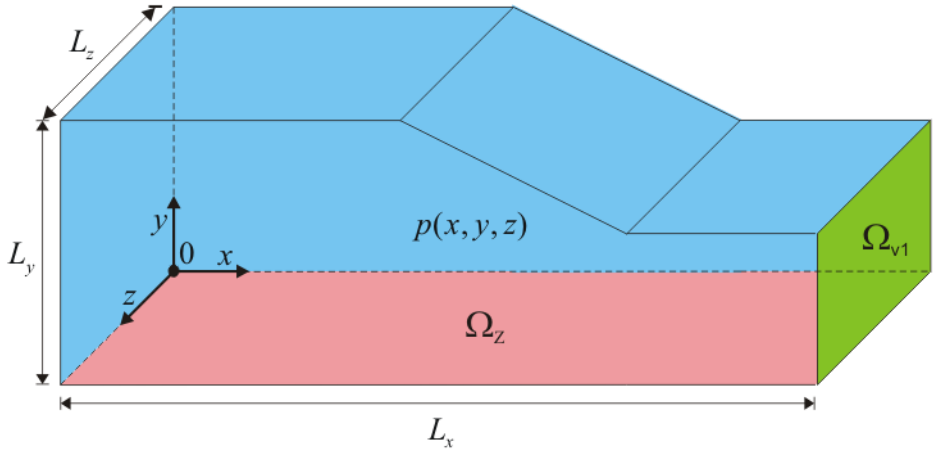

Figure 1: 3D acoustic problem

2.2 Domain decomposition

The considered 3D acoustic problem as shown in Figure 1 is non-convex. Therefore the problem domain V must be decomposed into at least two convex sub-domains [1], [5]. Figure 2 show three convex sub-domains $V_1 = \left(L_{x_1}, L_{y_1}, L_{z_1}\right) = (1.8, 1.4, 1.7)\,m$, $V_2 = \left(L_{x_2}, L_{y_2}, L_{z_2}\right) = (1.2, 1.4, 1.7)\,m$ and $V_3 = \left(L_{x_3}, L_{y_3}, L_{z_3}\right) = (1.02, 0.8, 1.7)\,m$. Notice that $V_1 \cup V_2$ is also a convex sub-domain, therefore it is not necessary to decompose this sub-domain and is only done to make the principle more clear.

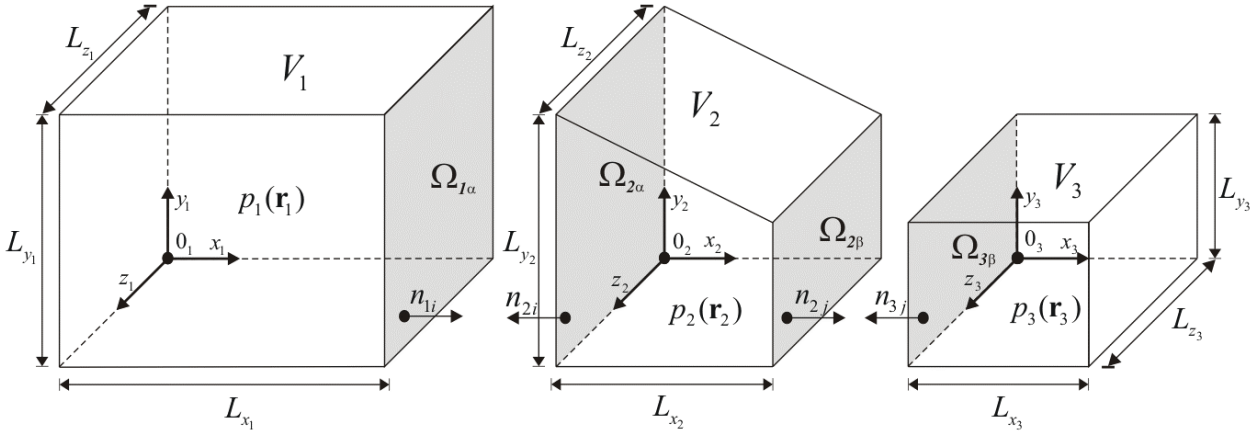

Figure 2: domain decomposition of a 3D non-convex acoustic problem into for instance three convex sub-domains

To couple the three sub-domains at the interfaces $\Omega_{1\alpha} = \Omega_{2\alpha}$ and $\Omega_{2\beta} = \Omega_{3\beta}$, pressure and normal velocity continuity conditions are enforced and the subindex i, j denotes the boundary surfaces

$$p_1(\mathbf{r}_1) = p_2(\mathbf{r}_2), \quad \frac{j}{\rho\omega}\frac{\partial p_1(\mathbf{r})}{\partial n_{1\alpha}} = \frac{j}{\rho\omega}\frac{\partial p_2(\mathbf{r}_2)}{\partial n_{2\alpha}}, \quad \forall \mathbf{r}_{1,2} \in \Omega_{1\alpha,2\alpha} \tag{5}$$

$$p_2(\mathbf{r}_2) = p_3(\mathbf{r}_3), \quad \frac{j}{\rho\omega}\frac{\partial p_2(\mathbf{r})}{\partial n_{2\beta}} = \frac{j}{\rho\omega}\frac{\partial p_3(\mathbf{r}_3)}{\partial n_{3\beta}}, \quad \forall \mathbf{r}_{2,3} \in \Omega_{2\beta,3\beta} \tag{6}$$

An alternative way to impose interface continuity is given in [4].

2.3 Pressure response approximation

The WBT is based on an indirect Trefftz approach and utilizes approximation solutions, which satisfy the governing differential equation exactly. In its application to the considered 3D acoustic problem, the pressure in cavity V_1 is approximated as an expansion $\hat{p}_1(\mathbf{r}_1)$, which is an expansion of n_{a_1} wave functions $\Phi_{a_1}(\mathbf{r}_1)$, the pressure in cavity V_1 is approximated as an expansion $\hat{p}_2(\mathbf{r}_2)$, which is an expansion of n_{a_2} wave functions $\Phi_{a_2}(\mathbf{r}_2)$ and the pressure in cavity V_3 is approximated as an expansion $\hat{p}_3(\mathbf{r}_3)$, which is an expansion of n_{a_3} wave functions $\Phi_{a_3}(\mathbf{r}_3)$.

$$p_l(\mathbf{r}_l) \approx \hat{p}_l(\mathbf{r}_l) = \sum_{a=1}^{n_{a_l}} \Phi_{a_l}(\mathbf{r}_l)\, p_{a_l} = \mathbf{\Phi}_l^T(\mathbf{r}_l)\mathbf{p}_l, \qquad l = 1,2,3 \tag{7}$$

where vectors $\mathbf{p}_l$ contain the unknown wave function contribution factors and $^{\mathbf{T}}$ denotes the transpose operator.

The acoustic wave functions Φ_{a_l} take one of the three following forms

$$\Phi_{a_l} = \begin{cases} \Phi_{a_{l_r}}(x,y,z) = \cos\left(k_{xa_{l_r}}x\right)\cos\left(k_{ya_{l_r}}y\right)e^{-jk_{za_{l_r}}z} \\ \Phi_{a_{l_s}}(x,y,z) = \cos\left(k_{xa_{l_s}}x\right)e^{-jk_{ya_{l_s}}}\cos\left(k_{za_{l_s}}z\right) \\ \Phi_{a_{l_t}}(x,y,z) = e^{-jk_{xa_{l_t}}}\cos\left(k_{ya_{l_t}}y\right)\cos\left(k_{za_{l_t}}z\right) \end{cases}. \tag{8}$$

Since the only requirement for the selection of the wave numbers $k_{xa_{l_m}}, k_{ya_{l_m}}$ and $k_{za_{l_m}}$ is that $k_{xa_{l_m}}^2 + k_{ya_{l_m}}^2 + k_{za_{l_m}}^2 = k^2$ with $l = 1,2,3$ and $m = r,s,t$, an infinite number of wave functions (8) can be defined for the expansions (7). It is proposed to select the following wave number components,

$$\begin{aligned} \left(k_{xa_{l_r}}, k_{ya_{l_r}}, k_{za_{l_r}}\right) &= \left(\frac{a_{l_1}\pi}{L_{x_l}}, \frac{a_{l_2}\pi}{L_{y_l}}, \pm\sqrt{k^2 - \left(\frac{a_{l_1}\pi}{L_{x_l}}\right)^2 - \left(\frac{a_{l_2}\pi}{L_{y_l}}\right)^2}\right) \\ \left(k_{xa_{l_s}}, k_{ya_{l_s}}, k_{za_{l_s}}\right) &= \left(\frac{a_{l_3}\pi}{L_{x_l}}, \pm\sqrt{k^2 - \left(\frac{a_{l_3}\pi}{L_{x_l}}\right)^2 - \left(\frac{a_{l_4}\pi}{L_{z_l}}\right)^2}, \frac{a_{l_4}\pi}{L_{z_l}}\right) \\ \left(k_{xa_{l_t}}, k_{ya_{l_t}}, k_{za_{l_t}}\right) &= \left(\pm\sqrt{k^2 - \left(\frac{a_{l_5}\pi}{L_{y_l}}\right)^2 - \left(\frac{a_{l_6}\pi}{L_{z_l}}\right)^2}, \frac{a_{l_5}\pi}{L_{y_l}}, \frac{a_{l_6}\pi}{L_{z_l}}\right) \end{aligned} \tag{9}$$

with $a_{l_1}, a_{l_2}, a_{l_3}, a_{l_4}, a_{l_5}, a_{l_6} = 0,1,2\ldots..$ L_{x_l}, L_{y_l} and L_{z_l} denote the dimensions of a rectangular prism enclosing (convex) sub-domain l.

2.4 Wave model

As mentioned before, the pressure approximations (7) satisfy a priori the governing Helmholtz equation (1). Only the boundary conditions (2), (3) and (4) and the interface continuity conditions (5) and (6) are violated. A square wave model is obtained by enforcing the pressure approximations to satisfy both the boundary conditions and the interface continuity conditions in a weighted residual or in a least-squares

integral sense. As shown in [7] the weighted residual formulation is more efficient and will therefore used in this and the following sections. The square wave model is given by

$$\begin{bmatrix} \mathbf{A}_{11}+\mathbf{C}_{11} & \mathbf{C}_{12} & \mathbf{0} \\ \mathbf{C}_{21} & \mathbf{A}_{22}+\mathbf{C}_{22} & \mathbf{C}_{23} \\ \mathbf{0} & \mathbf{C}_{32} & \mathbf{A}_{33}+\mathbf{C}_{33} \end{bmatrix} \begin{Bmatrix} \mathbf{p}_1 \\ \mathbf{p}_2 \\ \mathbf{p}_3 \end{Bmatrix} = \begin{Bmatrix} \mathbf{0} \\ \mathbf{0} \\ \mathbf{b}_3 \end{Bmatrix} \tag{10}$$

with vectors $\mathbf{p}_1$, $\mathbf{p}_2$ and $\mathbf{p}_3$ containing the unknown DOF's, i.e. the wave contribution factors, with sub-matrices $\mathbf{A}_{ii}(i=1,2)$, $\mathbf{C}_{ii}(i=1,2)$, $\mathbf{C}_{12}$, $\mathbf{C}_{21}$, $\mathbf{C}_{23}$ and $\mathbf{C}_{32}$ and vector

$$\mathbf{b}_3 = \int_{\Omega_{v1}} \mathbf{\Phi}_3 \overline{v}_n d\Omega \tag{11}$$

For the detailed description of the sub-matrices, the reader is referred to [5], [6].

The resulting system matrix in (10) is frequency dependent and almost fully populated with complex coefficients, but has a much smaller size as compared to corresponding FE models.

3 Basic concepts to consider vibration velocities

To extend the application field of the WBT methodology a new prescribed velocity boundary condition is introduced in order to consider the local distribution of vibration velocities (e.g. structural vibrations) at plane quadrilateral boundary surfaces. The velocity distributions can be derived from either measurement data (Laser Scanning Vibrometer) or from results of structural FEM analysis. By using this new boundary condition the excitation of the fluid due to local vibrations can be considered without loosing the advantages of computational efficiency of WBT but without taking into account the influence of the fluid to the local vibrations.

3.1 Problem definition

Consider a velocity distribution $\mathbf{v}(\mathbf{x},\omega)$ on a sub-domain Ω_v of the boundary of V, which is given at measurement points or simulation nodes $\mathbf{x_i}, i=1,...,n$. To incorporate this velocity boundary condition into the WBT-formulation of the problem, integrals of the form $\int_{\Omega_i} \mathbf{v_n} \psi_j d\Omega$ have to be numerically evaluated. This is realized with the Gaussian method, i.e. quadratures of the form are

$$\sum_{j=1}^{m} \mathbf{v_n}(\mathbf{y_j},\omega)\psi_j w_j \tag{12}$$

calculated for each circular frequency ω. Thus, for the numerical integration the velocity has to be known at the Gauss points $\mathbf{y_j}$, $j=1...,m$. To keep the quadrature efficient, it is preferable to distribute the Gauss points evenly at the unit square, which is obtained from the transformation of the surface Ω_i. Hence the gauss points on Ω_i itself are determined by the transformation of Ω_i onto the unit square. For that reason the Guass points can not be identified with the data points $\mathbf{x_i}, i=1,...,n$. Furthermore the amount of necessary Gauss points is related to ω and usually does not coincide with the number of data points. Therefore an algorithm that interpolates the velocity data given on a measurement or simulation mesh to all Gauss points $\mathbf{y_j}, j=1...,m$ is suggested.

3.2 Methodology

To realize the identification of the data at the given points $\mathbf{x_i}$ with the Gauss points $\mathbf{y_j}$ a method coming from the FEM was chosen. The set of data points is firstly defined with a mesh consisting of quadrilateral elements. For each Gauss point the closest element is identified. The data at the corners of the element is interpolated on the Gauss point. The elements of the data mesh are treated as finite elements for the identification of the closest element to a given Gauss point and for the interpolation of the velocity data. The shape functions $N_k\left(\xi_j,\psi_j\right)$ of the elements are used for the data interpolation

$$\hat{\mathbf{v}}_\mathbf{j} = \sum_{k=1}^{N} \mathbf{v_i} N_k\left(\xi_j,\psi_j\right). \tag{13}$$

The order of the interpolation accuracy $\left\|\mathbf{v_j} - \hat{\mathbf{v}}_\mathbf{j}\right\|$ is given by the order of the finite elements. The local coo-ordinates $\left(\xi_j,\psi_j\right)$ related to $\mathbf{y_j}$ are determined via the relationship

$$\mathbf{y_j} = \sum_{i=1}^{N} \mathbf{x_i} N_k\left(\xi_j,\psi_j\right). \tag{14}$$

The Gauss point is contained inside an element only if $\left|\xi_j\right| < 1, \left|\psi_j\right| < 1$. In that situation the correct element is found for $\mathbf{y_j}$. The method also applies to Gauss points outside the data mesh. In that case the identification is given by the element with the shortest distance $\max_i\left\{\left|\xi_i\right|, \left|\psi_i\right|\right\}$ to a given point $\mathbf{y_j}$.

The identification is not necessarily definite for the elements. A Gauss point lying on an edge between two elements ca be assigned to both elements. The realized algorithm terminates the identification process for $\mathbf{y_j}$ as soon as a matching element is found.

A for example quadrilateral linear Lagrange element is considered [8]. This element is given by the shape functions

$$N_k\left(\xi,\psi\right) = \frac{1}{4}\left(1+\xi_o\right)\left(1+\psi_o\right). \tag{15}$$

with $\xi_o = \xi\cdot\xi_k,\ \psi_o = \psi\cdot\psi_o,\ \left(\xi_k,\psi_k\right) \in \left\{(-1,-1),(-1,1),(1,-1),(1,1)\right\}$. The co-ordinates of $\mathbf{y_j}$ in the local FE-co-ordinate system are given by

$$\mathbf{y_j} = \sum_{k=1}^{4} \mathbf{x_{i,k}} N_k\left(\xi_j,\psi_j\right). \tag{16}$$

with the element nodes $\mathbf{x_{i,k}},\ k \in \left\{1,\ldots,4\right\}$. This gives a semilinear equation system

$$\mathbf{b_i}\xi_j + \mathbf{c_i}\psi_j + \mathbf{d_i}\xi_j\psi_j = 4\mathbf{y_j} - \mathbf{a_i}. \tag{17}$$

with the parameters

$$\begin{aligned}
\mathbf{a_i} &= +\mathbf{x_{i,1}} + \mathbf{x_{i,2}} + \mathbf{x_{i,3}} + \mathbf{x_{i,4}} \\
\mathbf{b_i} &= -\mathbf{x_{i,1}} + \mathbf{x_{i,2}} + \mathbf{x_{i,3}} - \mathbf{x_{i,4}} \\
\mathbf{c_i} &= -\mathbf{x_{i,1}} - \mathbf{x_{i,2}} + \mathbf{x_{i,3}} + \mathbf{x_{i,4}} \\
\mathbf{d_i} &= +\mathbf{x_{i,1}} - \mathbf{x_{i,2}} + \mathbf{x_{i,3}} - \mathbf{x_{i,4}}
\end{aligned}. \tag{18}$$

The equation system has to be solved to obtain ξ_j, ψ_j. In the more general case where the data mesh does not coincide with the surface Ω_v, an optimization problem of the following form has to be solved:

$$\left(\xi_j, \psi_j\right) = \arg\min_{\xi,\psi} \left\| \mathbf{b_i}\xi_j + \mathbf{c_i}\psi_j + \mathbf{d_i}\xi_j\psi_j - \left(4\mathbf{y_j} - \mathbf{a_i}\right) \right\|_2 . \tag{19}$$

4 Validation example

4.1 Problem description and measurement setup

The test setup (Sound Brick) was especially developed for validation purpose. In geometry, it resembles a simplified car cavity with engine bay. The walls are made out of concrete with a special surface treatment to ensure acoustically rigid boundary conditions. At the front side, a 2mm steel plate is fixed on the Sound Brick over an additional frame and is excited with a shaker (Figure 3). On the complete floor, a fire resistant foam (Melamin 50mm) is applied as damping material.

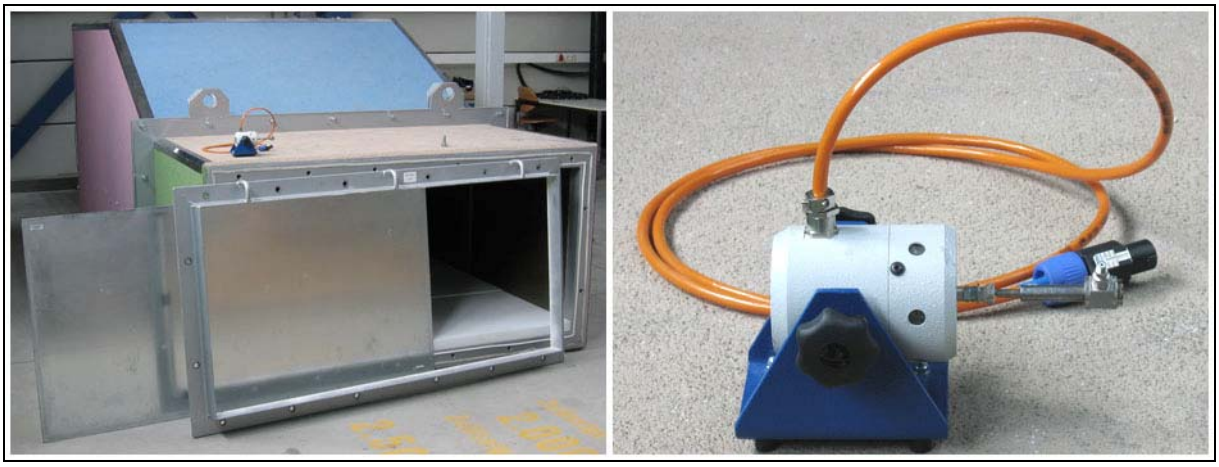

Figure 3: Sound Brick with damping material on the floor, 2mm steel plate and frame to fix the plate on the front side (left figure). Shaker to excite the steel plate (right figure).

The measurement setup, to measure the pressure frequency response function at the position MIC 1 (0.51/0.425/0.5m) due to the shaker excitation at the position (4.02/0.20/0.35m) is shown in Figure 4.

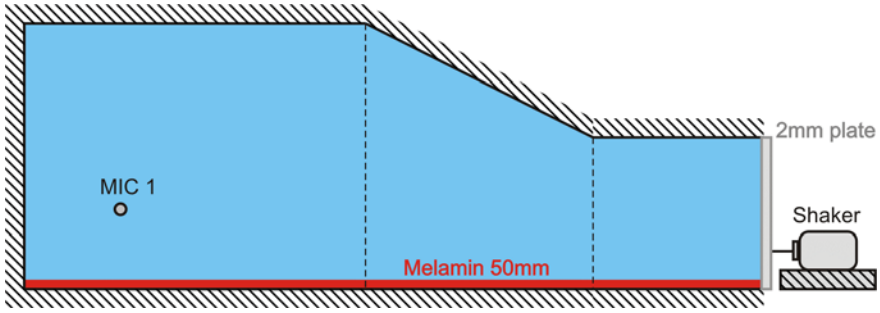

Figure 4: Sound Brick measurement setup to measure the pressure frequency response function (FRF) at position MIC 1 due to the shaker excitation on the 2mm steel plate.

In Figure 5, the measurement setup for measuring normal velocity frequency response functions on the 2mm steel plate due to the shaker excitation with the Laser Scanning Vibrometer, is shown. In order to loose no measurement points on the plate during the Laser Scanning, the shaker is positioned inside the Sound Brick. The back panel of the Sound Brick is opened, since the effect of the fluid to the structural behavior can be neglected.

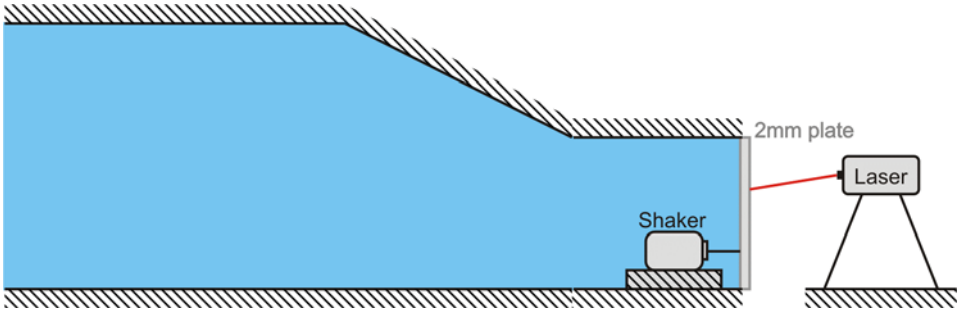

Figure 5: Sound Brick measurement setup to measure the normal velocity frequency response functions (FRF's) at 231 positions on the 2mm steel plate with the Laser Scanning Vibrometer.

With the Laser Scanning Vibrometer, Polytec PSV 200 (Figure 6), a constant Laser-point-mesh of 21x11=231 points have been measured. Notice the Figure 6 shows only a default video picture of a Laser-point-mesh.

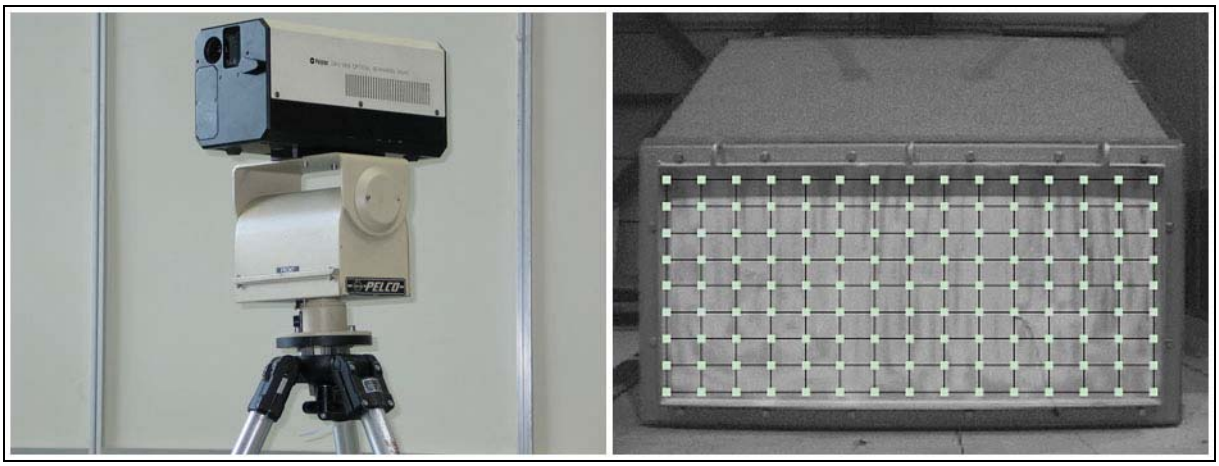

Figure 6: Laser Scanning Vibrometer, Polytec PSV 200 (left figure) and a default video-picture of the scanned points on the steel plate (right figure).

The damping material (Illbruck plano – Melamin 50mm) is used as a normal impedance which is determined in an impedance measurement tube. After smoothing and interpolating this complex data (see Figure 7) it is ready to be used in the numerical model.

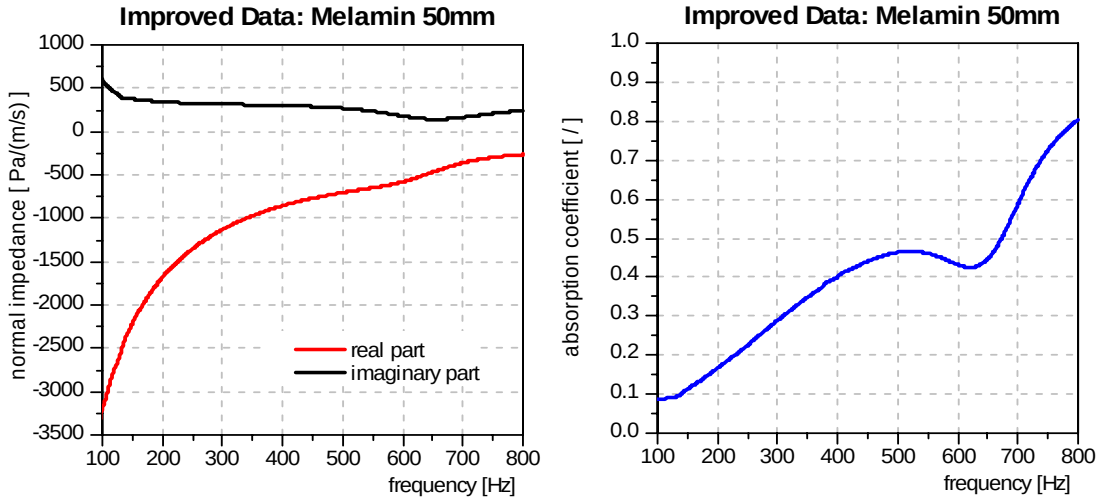

Figure 7: Smoothed and interpolated measurement data of the damping material (Melamin 50mm – left figure) and the corresponding absorption coefficient (right figure).

4.2 Comparing measurements and simulation results

The results of the measurements described in section 4.1 were compared to simulated ones. As an example, results of response point MIC 1 (position 0.51/0.425/0.5m) and the excitation point on the plate (4.02/0.20/0.35m) are shown. The simulations were carried out by vibro-acoustic FEM on one hand and by WBT including the new local boundary condition for normal velocity, on the other. Three different comparisons of measured and calculated results were performed as follows.

4.2.1 Measurements (MM) – Finite Elements Method (FEM)

The Finite Element Model consists of a fluid mesh ($l_{\max} = 10cm$) and a structural mesh ($l_{\max} \approx 1cm$) with 270 (ident) coupling points and a unit force ($F = 1N$) excitation normal to the plate. The damping material is applied as a complex normal impedance surface on the floor.

Nr.	Structural Eigenvalues	Nr.	Structural Eigenvalues	Nr.	Fluid Eigenvalues
1	18.8 Hz	8	62.0 Hz	1	44.5 Hz
2	23.6 Hz	9	73.5 Hz	2	83.5 Hz
3	32.3 Hz	10	80.9 Hz	3	101.4 Hz
4	44.8 Hz	11	88.6 Hz	4	
5	49.5 Hz	12	95.6 Hz	5	
6	54.1 Hz	13	100.0 Hz		
7	61.0 Hz				

Table 1: Predicted FEM structural and fluid eigenvalues up to about 100 Hz.

Comparing predicted and measured pressure frequency response functions (FRF), Figure 8, the correlation was found rather poor. A possible effect of the number of nodes for coupling the fluid and the structural meshes was found of minor effect. A good correlation of the fluid and structural natural frequencies can be observed, too (see Table 1 and peaks in measured results of Figure 8). However, comparing structural vibration from tests and FEM calculations, it could be seen, that the boundary condition of the structural model, assumed as totally fixed at the edges, is not adequate. As a costly identification of boundary conditions for the FEM model is of less priority, the investigations were continued by comparing FEM and WBT simulation results on one hand and those of test and WBT on the other.

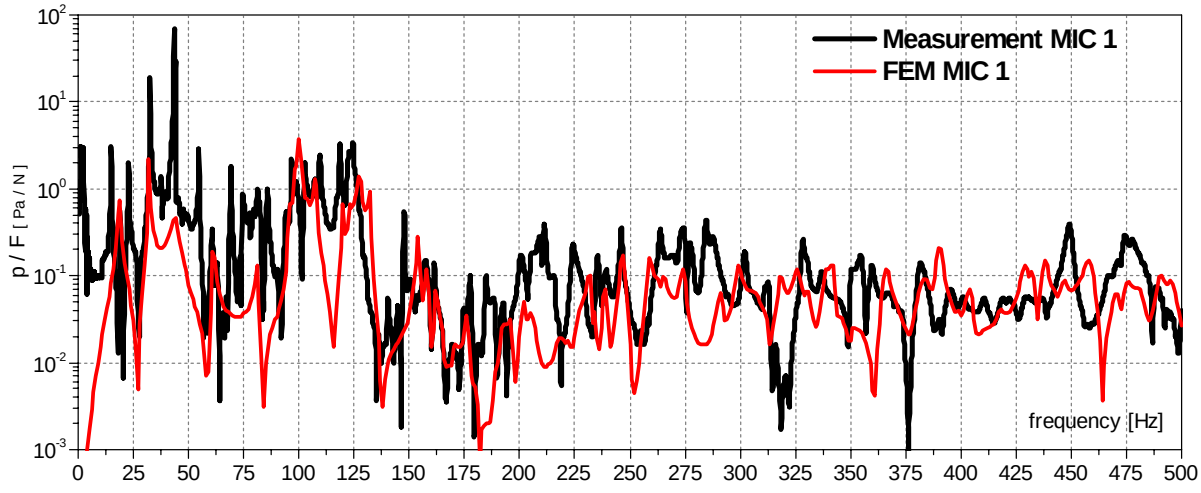

Figure 8: Comparison of the amplitudes of pressure FRF [Pa/F] of the measurements (black curve) and the FEM prediction (red curve) in response point MIC 1.

4.2.2 Wave Based Technique (WBT(FEM)) – Finite Elements Method (FEM)

Using velocity contributions on the plate calculated with the FEM as a boundary condition for the WBT (see section 3.2), the pressure frequency response functions correlate quite well with standard FEM prediction (as described in 4.2.1), Figure 9. Herein, 16577 single velocity results were taken into account to perform the new boundary condition for locally distributed normal velocities with the WBT.

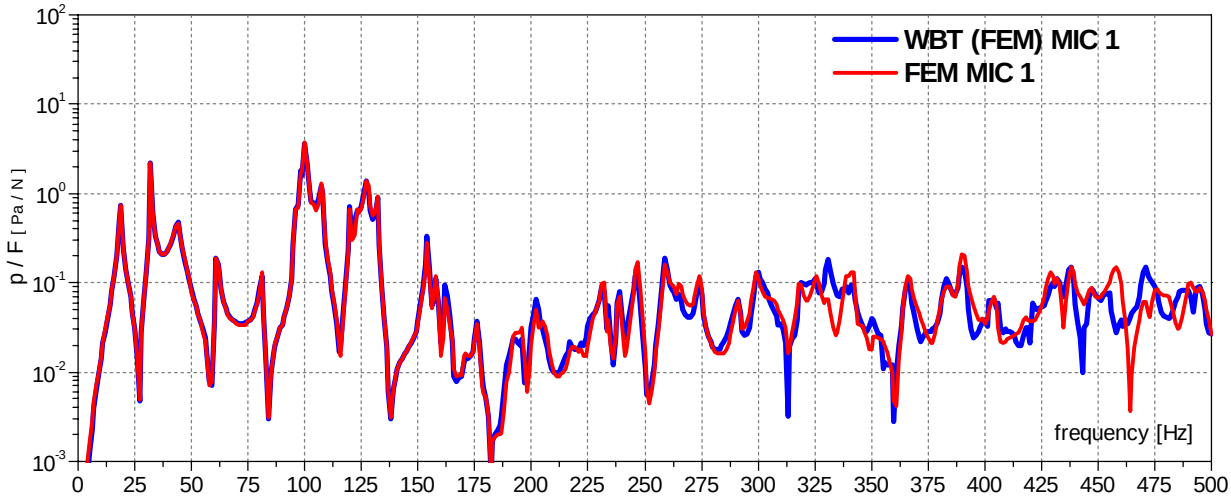

Figure 9: Comparison of the amplitudes of pressure FRF [Pa/F] of the FEM prediction (red curve) and the WBT(FEM) prediction (blue curve) in response point MIC 1.

4.2.3 Measurements (MM) – Wave Based Technique (WBT(MM))

The WBT prediction in this section was performed with normal velocities measured at 231 points on the plate with the Laser (see Figure 6), according to the method described in section 3.2. Figure 10 shows comparison of results from measurement and WBT prediction for the response point MIC 1.

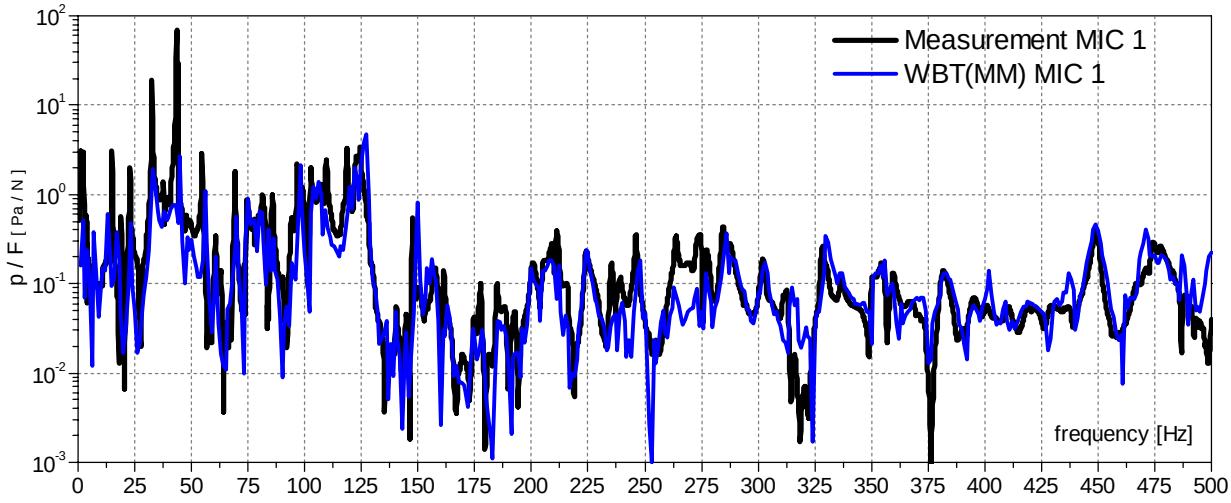

Figure 10: Comparison of the amplitudes of pressure FRF [Pa/F] of the measurements (black curve) and the WBT(MM) prediction (blue curve) in response point MIC 1.

The resonance frequencies in Figure 10 are predicted accurately over the whole frequency range. The amplitudes up to 50 Hz are underestimated, which might be caused by the low power of the small shaker used for the test. In the frequency range between 50 and 500 Hz, the WBT prediction fits quiet well to the measurement results.

The WBT simulations were carried out on a PC-Windwos platform, using a Fortran90 implementation developed by ACC. The FEM simulations are performed on the same platform with MSC Nastran 2004. Table 2 summarizes the computational resources, the model sizes and CPU times of the applied models. Note that, due to the applied implementation, all WBT simulations are performed with a constant number of wave functions over the frequency range and sub-domains. This number is determined by the highest frequency of interest and by the biggest sub-domain. As a consequence, the WBT predictions at lower frequencies could be accelerated, since, in this frequency region less wave functions are required to have accurate predictions. This is one of the subjects to further research.

Intel Pentium IV 1Gbyte RAM 3 GHz CPU	**FEM** (10cm) MSC Nastran SOL 111	**FEM** (5cm) MSC Nastran SOL 111	**WBT(FEM)**	**WBT(MM)**
Fluid	12095 nodes	90054 nodes	450 WF	450 WF
Structure	16577 nodes	16577 nodes	16577 points	231 points
Total DOF's	94980	172939	450	450
CPU time [min]	66	253	36	34

Table 2: model diagnostics

5 Conclusions

This paper discusses the application of the Wave Based Technique for the analysis of a multi-domain 3D acoustic cavity considering forced excitation at boundaries and effects of absorption materials. The new boundary condition for local velocity contributions allows a simulation of vibro-acoustic problems with the WBT-Fluid implementation. The velocity distributions can be derived from either measurement data or from results of structural FEM analyses.

The comparison of the results from WBT predictions, FEM predictions and measurements confirm the quality of the WBT in a real test application considering effects of absorbing material. Furthermore, the high computational efficiency of the WBT compared to FEM could be proven, which allows it to produce more accurate prediction results in the mid-frequency range at reasonable computational cost.

Acknowledgements

The authors would like to thank Prof. Wim Desmet of the Departement of Mechanical Engineering, division PMA, K.U. Leuven and his colleagues for the support and co-operation in the research work described. Moreover, the work was supported and funded by AVL List GmbH, Graz and MAGNA STEYR FAHRZEUGTECHNIK, Graz. Finally, the work was funded by the Austrian government, the government of Styria and the city of Graz.

References

[1] W. Desmet, *A wave based prediction technique for coupled vibro-acoustic analysis*, Phd Thesis, K.U. Leuven, division PMA, Leuven (1998).

[2] A. Hepberger, *Mathematical methods for the prediction of the interior car noise in the middle frequency range*, Phd Thesis, TU Graz (2002).

[3] E. Trefftz, *Ein Gegenstück zum Ritzschen Verfahren*, Proceedings of 2nd International Congress on Apllied Mechanics, Zürich (1926), pp. 131-137.

[4] B. Pluymers, W. Desmet, D. Vandepitte, P. Sas, *A Trefftz-based prediction technique for multi-domain steady-state acoustic problems*, Proceedings of the 10th International Congress of Sound and Vibration ICSV10, Stockholm (2003)

[5] A. Hepberger, B. Pluymers, K. Jalics, H.-H. Priebsch, W. Desmet, *Validation of a Wave Based Technique for the analysis of a multi-domain 3D acoustic cavity with interior damping and loudspeaker excitation*, Proceedings of the 33rd International Congress and Exposition on Noise Control Engineering, Prague (2004).

[6] B. van Hal, A. Hepberger, H.-H. Priebsch, W. Desmet, P. Sas, *High performance implementation and conceptual development of the wave based method for steady-state dynamic analysis of acoustic problems*, Proceedings of ISMA 2002, Vol. II, Leuven (2002), pp. 817-826.

[7] A. Hepberger, H.-H. Priebsch, W. Desmet, B. van Hal, B. Pluymers, P. Sas, *Application of the Wave Based Method for the Steady-state Acoustic Response Prediction of a Car Cavity in the Mid-frequency Range*, Proceedings of ISMA 2002, Vol. II, Leuven (2002), pp. 877-884.

[8] F. Diwoky, *Development of a methodology to numerically simulate the vibro-acoustic properties of exhaust systems*, Phd Thesis, TU Graz, Graz (2003)